CNR-INO
ISTITUTO NAZIONALE DI OTTICA
CONSIGLIO NAZIONALE DELLE RICERCHE

EURONNAC4 Special Topics workshop 2022
La Biodola Bay, Isola d'Elba, Italy
18-24 september 2022

kHz rep rate, kW average power class laser development with Tm-based ceramics

L. Labate[1], F. Baffigi[1], G. Cellamare[1], D. Palla[1], A. Pirri[2], G. Toci[3], M. Vannini[3], L.A. Gizzi[1]

[1]Consiglio Nazionale delle Ricerche (CNR), Istituto Nazionale di Ottica, Pisa, Italy

[2]Consiglio Nazionale delle Ricerche (CNR), Istituto di Fisica Applicata "N. Carrara", Sesto Fiorentino (FI), Italy

[3]Consiglio Nazionale delle Ricerche (CNR), Istituto Nazionale di Ottica, Sesto Fiorentino (FI), Italy

www.ino.cnr.it

Context: high average power ultrashort lasers for LWFA

EuPRAXIA CDR

The EuPRAXIA laser(s)

Quantity	Baseline Value
Laser 1 - Energy on target	$\leq$ 5–7 J
Laser 1 - Pulse duration	$\geq$ 20–30 fs
Laser 2 - Energy on target	$\leq$ 15–30 J
Laser 2 - Pulse duration	$\geq$ 20–30 fs
Laser 3 - Energy on target	$\leq$ 50–100 J
Laser 3 - Pulse duration	$\geq$ 50–60 fs
Wavelength	800 nm
Repetition rate	20–100 Hz
Energy stability (RMS)	0.6–1 %
Pointing stability (RMS)	$\sim$1 μrad

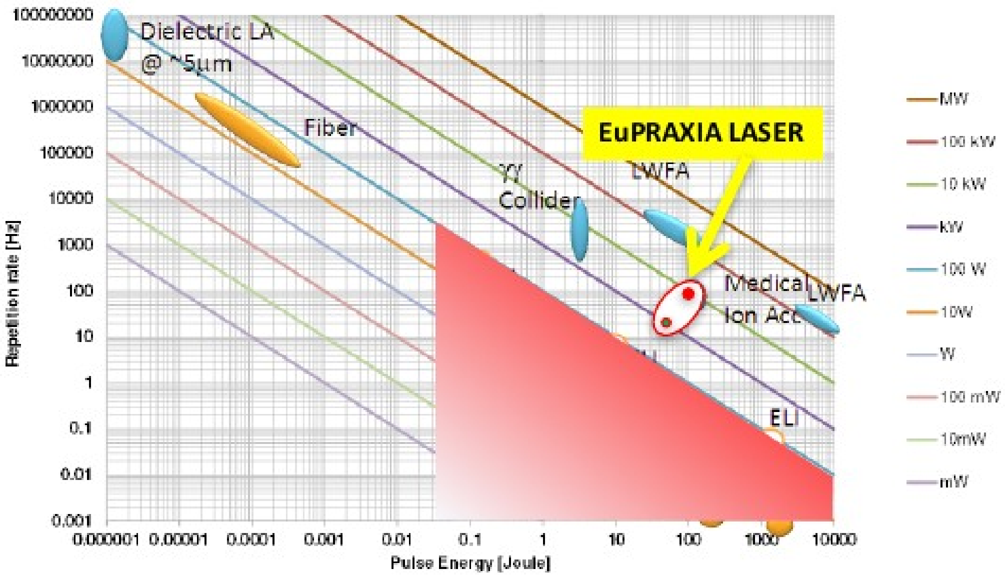

Average power ranging from 1kW to 10kW

Laser technologies for future accelerators. The Multi-Pulse extraction scheme

Report on Laser Technologies for kBELLA and beyond (2017)

2.C. Laser technology for a long-term 10 GeV, 100 kHz LPA collider module

- TiSa with incoherently combined pump lasers
- TiSa with diode pumped pump lasers (thick or thin disk)
- Tm:YLF with direct pumping CPA
- Fiber-based lasers with coherent combining

Due to efficiency limitations, TiSa-based technologies unlikely to go beyond the ~kW average power (could be used for injector stage or as single stage LPA for future light sources)

Tm based materials with Multi-Pulse Extraction (*this work*)

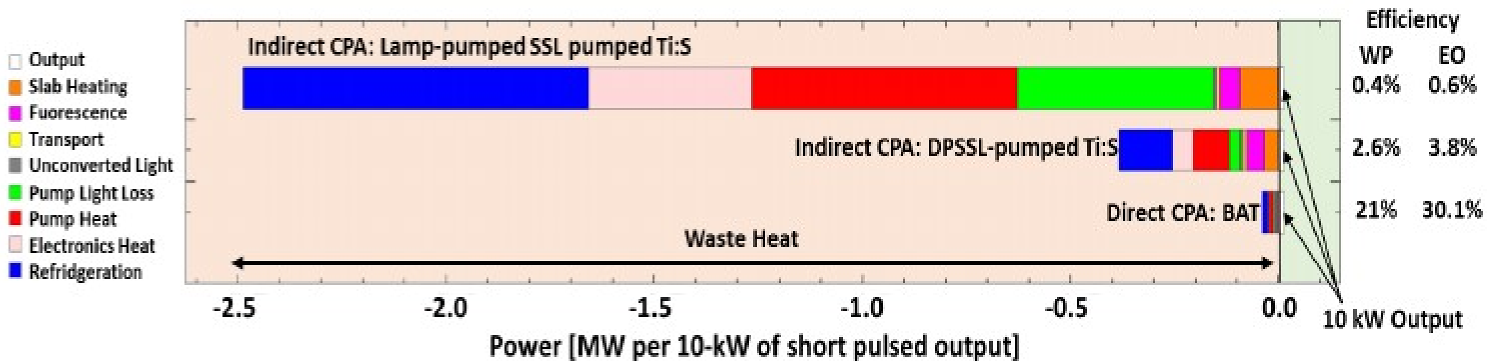

C. Siders et al., EAAC 2017

Multi-Pulse Extraction
- energy is stored over long (life)times (comparable to the inverse of the rep rate)
- possibility of (quasi)CW pumping, possibly with commercial diodes
- extraction fluence can be much lower than in SPE schemes (possibly affecting the B-integral, ...)
- allows the usage of high saturation fluence materials → direct pumping, lower QD, ...

High average power laser development at CNR Pisa

"ELITE" infrastructure @ CNR-INO Pisa

- grounded on the Intense Laser Irradiation Laboratory (ILIL), currently operating a 200TW system
- aimed at commissioning a new experimental area devoted to laser-driven particle acceleration with a strong focus on medical applications (mid-term applications of kHz rep rate, kW av power systems: biomedical imaging, FLASH radiotherapy, ...), thus requiring high average flux particles/photons flux

In this framework, the development of a high average power, ultrashort laser system is also being carried out (jointly funded through the "APOLLO" project), using a MPE architecture with ceramic materials

APOLLO system design specs: pulse duration ~50-100fs (potential), pulse energy > 500mJ, repetition rate 1kHz

Outline of this talk

- Sesquioxides ceramic materials
- Overview of the system architecture
- Current design status: System modelling
    - optical gain modelling
    - pumping scheme
    - thermomechanics
    - atomic dynamics of Multi-Pulse Extraction
- Ceramic Tm:Lu2O3 sample experimental characterization
    - Absorption spectrum (at the pump wavelength)
    - Lasing properties

Laser materials

Most common host matrices
- Garnets, X3Z2(SiO4)3,
  Y3Al5O13 (YAG); Lu3Al5O12 (LuAG), Gd3Ga5O12 (GGG), ...
- Fluorinated
  LiYF4 (YLF), CaF2, LuLiF4, ...
- Vanadates, VO3-4
  YVO4, GdVO4, LuxGd1-x(VO)4...
- Sesquioxides, X2O3
  Lu2O3, Sc2O3, Y2O3
- Others

Yb3+, Tm3+ dopants

Direct pumping with diode lasers ⇨ High efficiency

Long upper-state lifetime ⇨ High energy storage capability

Small ionic diameter ⇨ Several possible hosts with different properties; heavy doping allowed

Broad absorption band ⇨ Tunable emission

Broad emission band ⇨ Ultrashort pulses generation

New materials: CERAMICS vs CRYSTALS

In 2003 the first laser oscillation in YAG ceramic

K. Takaichi *et al.* "Yb^{3+}doped $Y_3Al_5O_{12}$ ceramics a new solid-state laser material", Phys. Status Solid A 200, R5-7 (2003

Higher dopand concentration and more uniform distribution;

Easier to fabricate and less expensive (lower processing temperature and shorter processing time);

Stronger fracture toughness (Ex. In YAG ceramic 5 time higher than in the corresponding crystal)*;

* A. A. Kaminskii *et al.*, Crystollogr. Rep. 50 (5), 1611161, (2005)

CNR-INO

A. Pirri et al., Materials 15, 2084 (2022)

Courtesy of A. Pirri

THERMAL CONDUCTIVITY

Thermal conductivity in W/m/K of different sesquioxide crystals in comparison to YAG with and without Yb-doping. Values in [] are estimated.

Temperature	30°C	50°C	60°C	70°C	80°C	90°C	100°C
Sc_2O_3	[16.5]	15.5	14.9	14.4	13.9	13.6	13.3
Yb(2.8%):Sc_2O_3	6.6	6.4	-	6.5	-	-	6.3
Y_2O_3	[13.6]	12.8	12.4	12.0	11.6	11.2	10.8
Yb(2.7%):Y_2O_3	7.7	7.4	-	7.2	-	-	6.8
Lu_2O_3	[12.5]	12.2	11.9	11.6	11.2	10.8	10.3
Yb(2.7%):Lu_2O_3	11.0	10.8	10.7	10.6	10.3	10.1	9.8
YAG	11	-	-	9.2	-	-	8.4
Yb(5%):YAG	6.8	-	-	6.3	-	-	6.0

R. Peters et al., *Appl Phys B Lasers Opt*. 102(3), 509, (2011; U. Griebner et al.,Opt. Express 12(14), 3125 (2004)

The thermal conductivity depends on the host and decrease by increasing the doping concentration. **Undoped sesquioxides show the highest values.** Moreover, in matrices contening Lu3+ it is not affected by doping levels.

A. Pirri et al., Materials 15, 2084 (2022)

Courtesy of A. Pirri

Active medium selection

Possible Tm hosts

laser host material	σ_{abs} (10^{-21} cm^2)	λ_{em} (nm)	σ_{em} (10^{-21} cm^2)	λ_{th} (W m^{-1} K^{-1})	τ (ms)	reference
YAG	7.5	2013	1.8	13	10	Heine, 1995
YLF	σ pol 3.6 π pol 8.0	1910 1880	2.35 3.7	6	15.6	Payne et al., 1992 Walsh et al., 1998
Lu_2O_3	3.8	2070 1945	2.3 8.5	13	3.8	Koopmann et al., 2009a

laser host material	λ_p (nm)	λ_{em} (nm)	cw output power (W)	slope eff. (%)	reference
YAG	805	2013	115	52	Honea et al., 1997
YAG	800	2013	120		LISA laser products OHG *
YLF	792	1910	55	49	Schellhorn, 2008
YLF	790	1912	148	32.6	Schellhorn et al., 2009
Lu_2O_3	796	2070	1.5	61	Koopmann et al., 2009a

[Scholle et al., 2010]

Selected material: *Tm:Lu2O3*

- Emission at 2 μm (eye-safe)
- Large amplification bandwidth
- Direct pumping at 800 nm, using diodes operating in (quasi) CW mode (available and scalable)
- Multi-pulse extraction at high repetition rate > 1 kHz; Ideal for accelerator technology
- Mature ceramic production technology

Overall architecture and amplifier(s) design

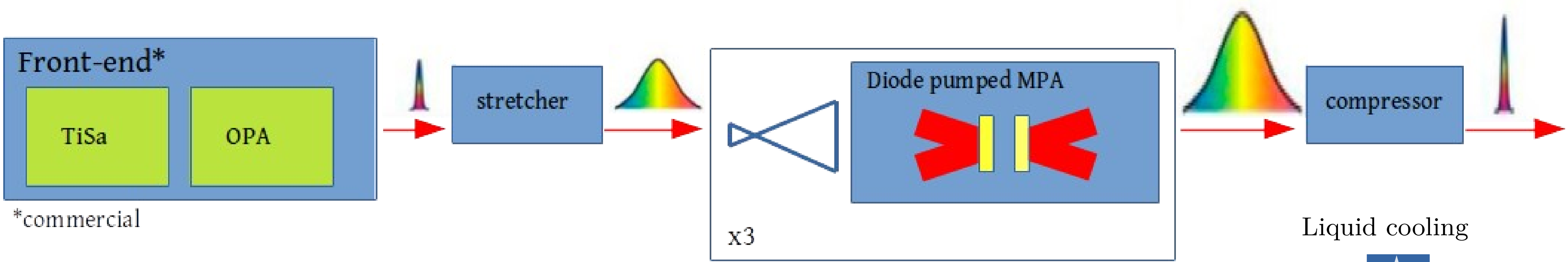

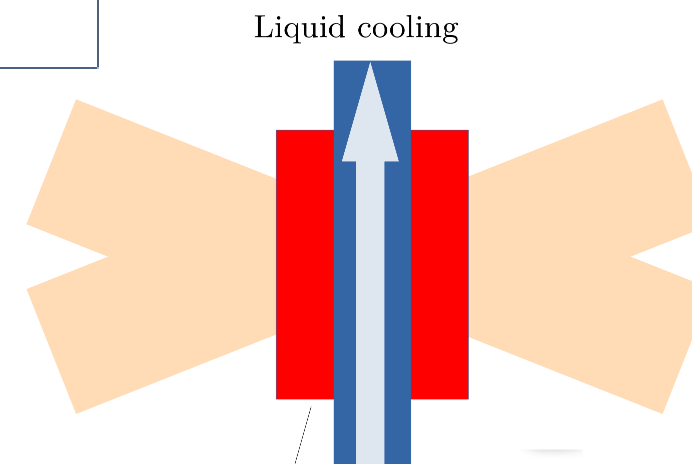

3 amplification stages, each based on a 2 active media multipass scheme.
Active mirror config, with cooling carried out on the rear side (tentative) or on both sides

Selected doping: 4% at

Pulse energy (goals/expected):
>1mJ seeding the 1st amp
~8 mJ seeding 2nd amp
>50mJ seeding the 3rd amp
~500mJ from 3rd amp

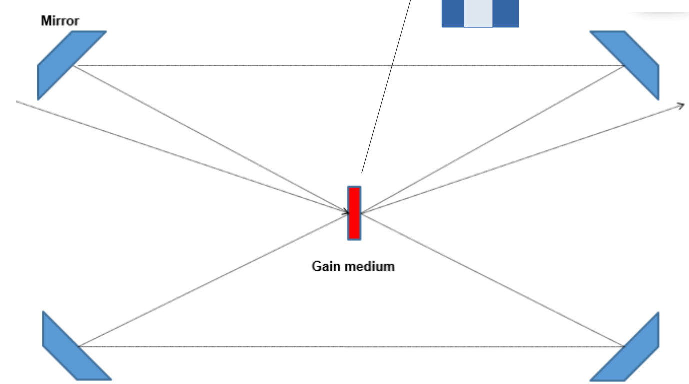

Amplifier concept: active mirror with edge pumping

Wide-Bandwidth Tm-Based Amplifier for Laser Acceleration Driver[a]

Drew A. Copeland[b], John Vetrovec , and Amardeep S. Litt
Aqwest LLC
Larkspur, CO USA

High Energy/Average Power Lasers and Intense Beam Applications VIII, edited by Steven J. Davis, Michael C. Heaven, J. Thomas Schriempf, Proc. of SPIE Vol. 9729, 97290I · © 2015 SPIE · CCC code: 0277-786X/15/$18 · doi: 10.1117/12.2220010

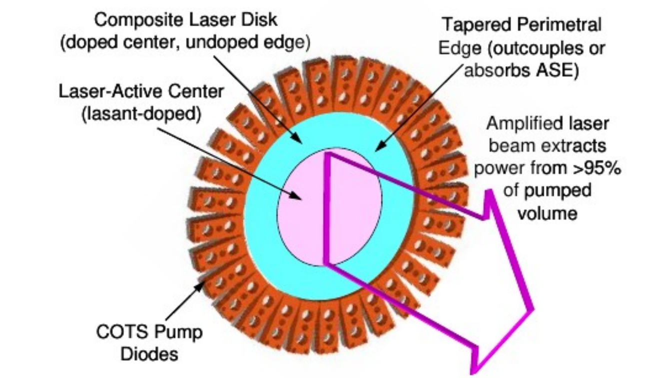

- *COTS pump diode arrays (multiple vendors)*
- *Diode-to-gain medium coupling efficiency >95%*
- *Pump absorption efficiency >90%*
- *Gain uniformity >90%*
- *Extraction from > 95% of pumped volume*
- *ASE absorption / outcoupling via tapered disk edge*
- *Round aperture for good mode matching*
- *Excellent optical quality ⇒ adaptive optics not necessary*
- *Disk can be either gas, liquid, or conductively cooled*
- *Very simple, compact, and lightweight packaging*

Figure 11. *Edge-pumped disk laser module uses standard commercial off-the-shelf (COTS) diodes closely coupled to the disk edge for high efficiency, uniform gain, and compact packaging.*

(a) Reflective disk (aka active mirror) – liquid cooled *(b) Transmissive disk – gas cooled*

Figure 4. *Architectures for cooling disk lasers.*

CNR-INO

3rd STAGE

	SEED DIAMETER (mm)	SEED PROFILE	PUMP DIAMETER (mm)	PUMP PROFILE	PUMP ENERGY DENSITY (J/m3)	TOTAL PUMP ENERGY (mJ)	INPUT ENERGY (mJ)	OUTPUT ENERGY (mJ)	NUMBER OF PASSES FOR EACH DISK	PEAK OF INTENSITY (W/m2)	PEAK OF FLUENCE (J/cm2)	EXTRACTION EFFICIENCY
STANDARD	8.5	SUPERGAUSSIAN OF ORDER 2	16	SUPERGAUSSIAN OF ORDER 5	3.00E+06	3600	56	508	35	2.4E+13	0.6	0.14
+5% PUMP ENERGY	8.5	SUPERGAUSSIAN OF ORDER 2	16	SUPERGAUSSIAN OF ORDER 5	3.2E+06	3780	56	563	35	2.58E+13	0.64	0.15
-5% PUMP ENERGY	8.5	SUPERGAUSSIAN OF ORDER 2	16	SUPERGAUSSIAN OF ORDER 5	2.90E+06	3420	56	456	35	2.2E+13	0.55	0,13

OUTPUT BEAM STANDARD CONFIGURATION

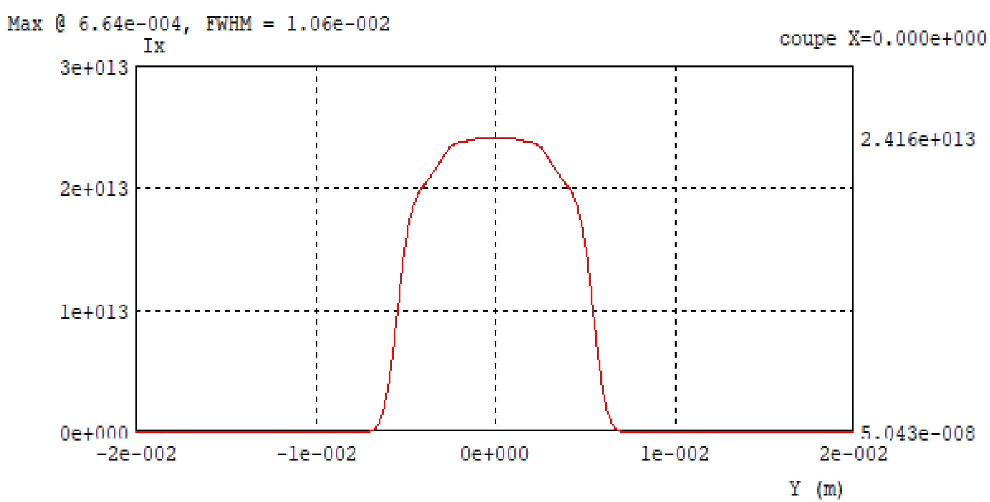

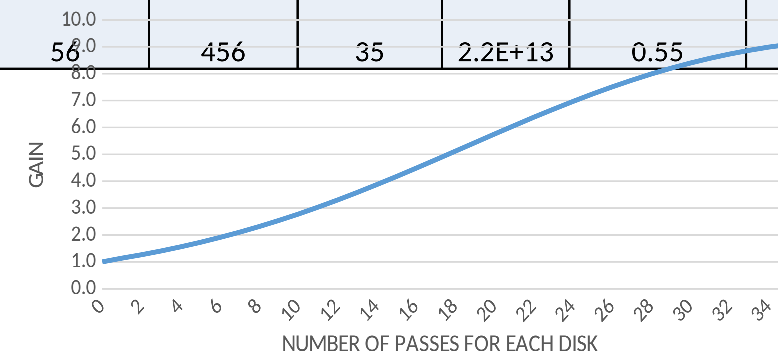

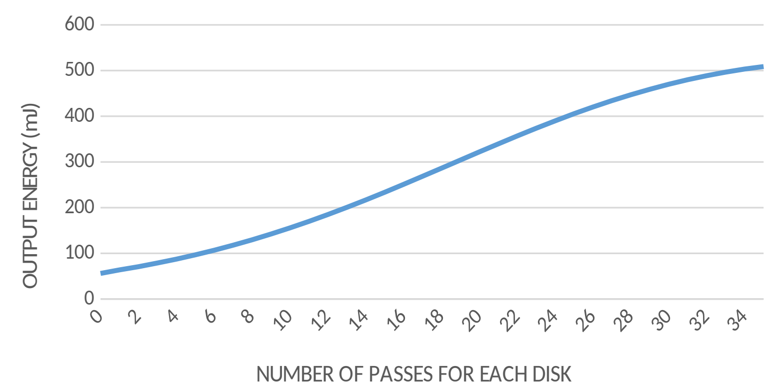

CNR-INO

Pumping ray-tracing: the general scheme

Ray-tracing code developed to model the pump absorption
Allows the pumping configuration (diode bars #/geometry, diode bars focusing/divergence, pump beam longitudinal reflection on surfaces, ...) to be optimized (in terms of overall pump energy absorption, transverse/longitudinal homogeneity, ...)
Doping longitudinal/transverse tailoring allowed

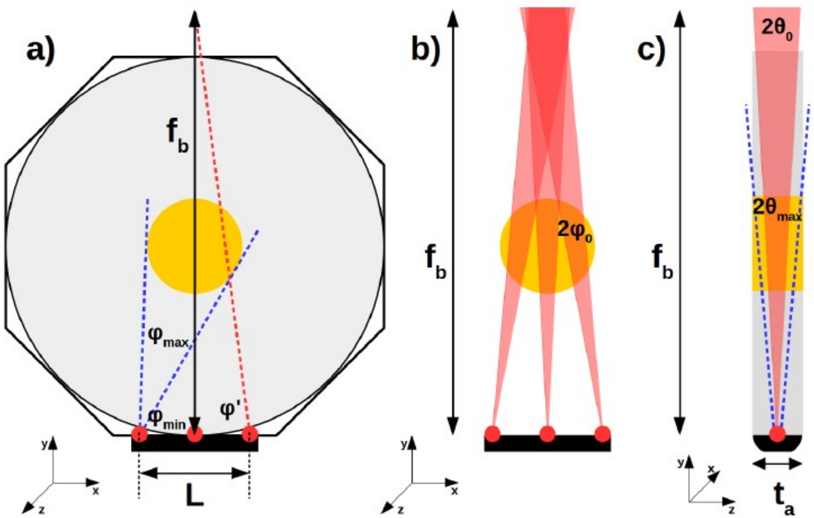

If the irradiation occurs through **optical fibers**, the model still holds (divergence angles depends on the numerical aperture).

Single Bar (3 subarray, directed at center)

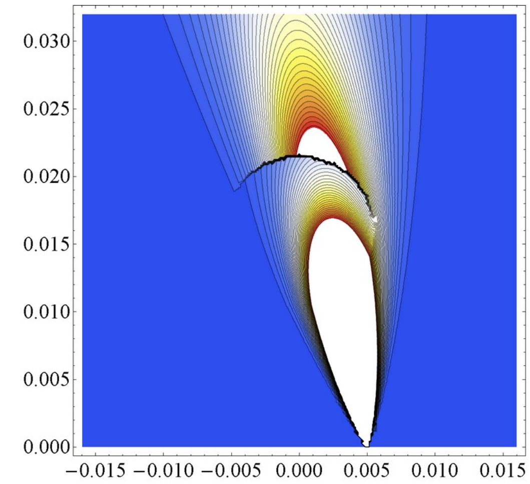

Total absorbed power density

$$Q(x,y,z)=\underbrace{\alpha(x,y,z)}_{|.|coeff.} I_A(x,y,z)$$

Optical power density

$$(1-\eta_h)Q(x,y,z)$$

Heat density

$$\eta_h Q(x,y,z)$$

D. Palla *et al*,, Opt. Laser Techn. 156, 108524 (2022)

Sample results (1st amp) for different "focusing" configurations

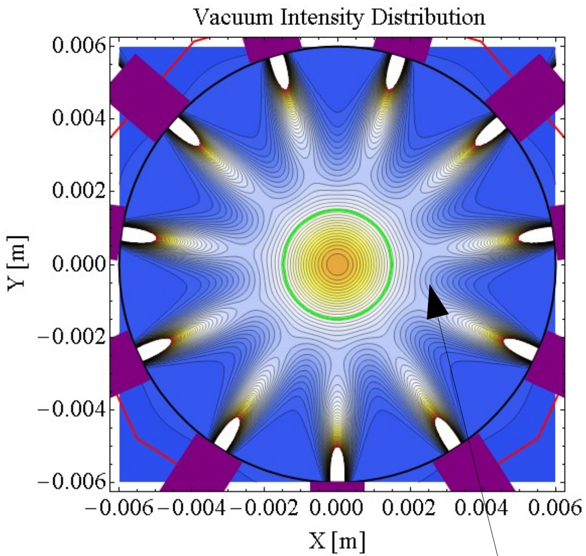

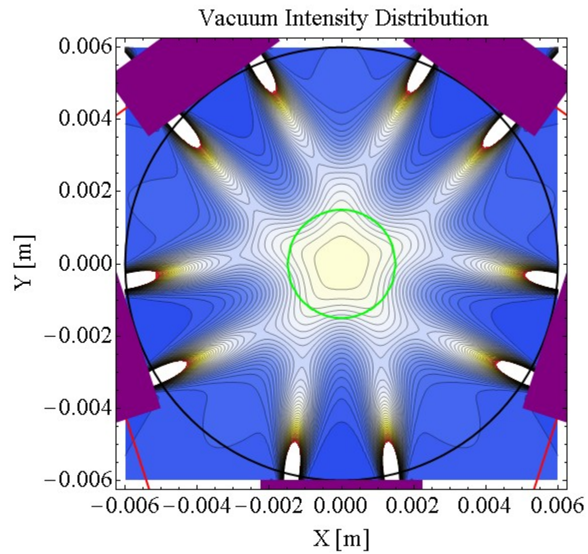

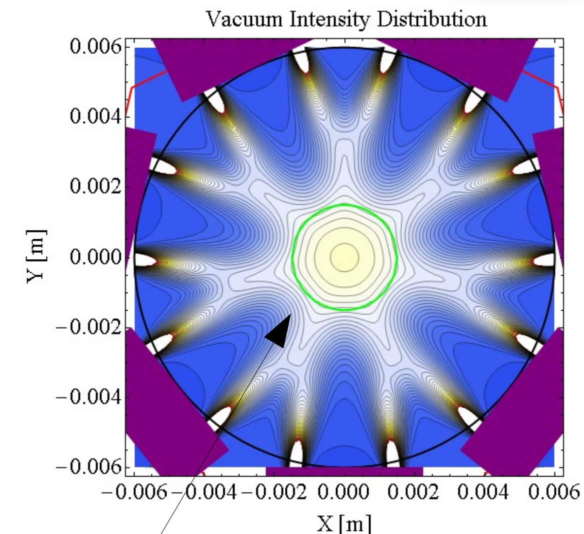

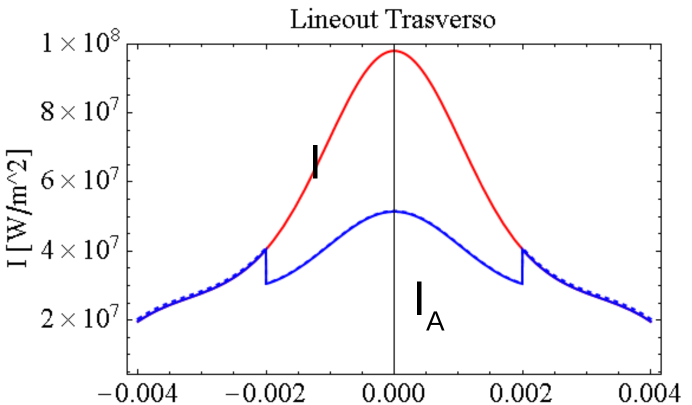

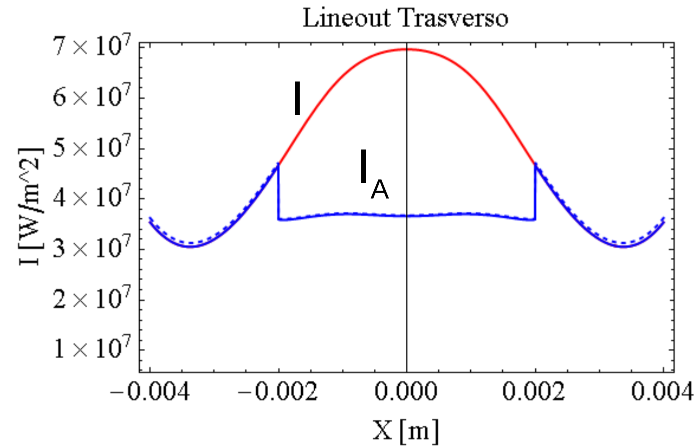

D. Palla *et al*,, Opt. Laser Techn. 156, 108524 (2022)

CNR-INO

Sample results for 3rd amp

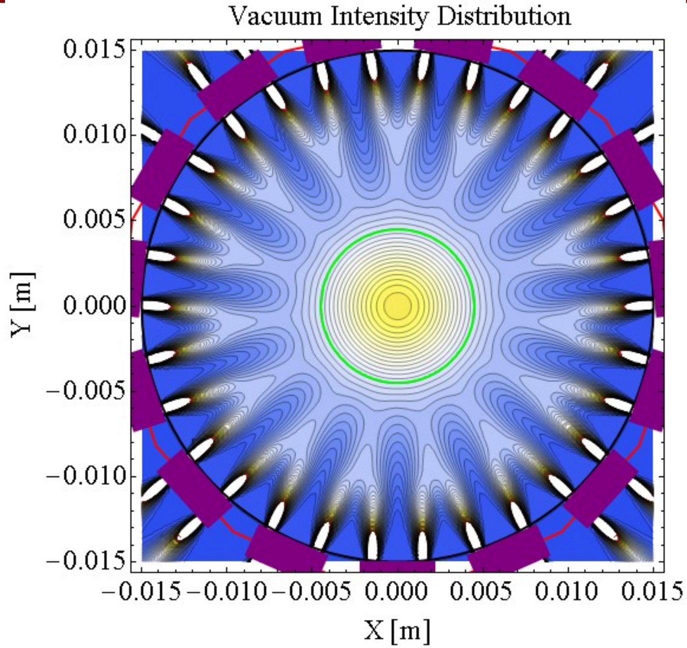

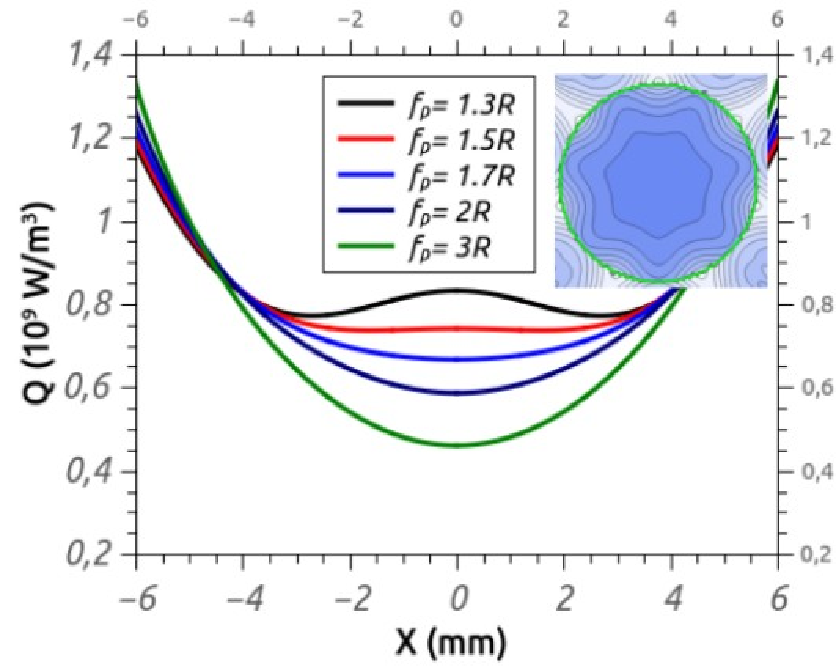

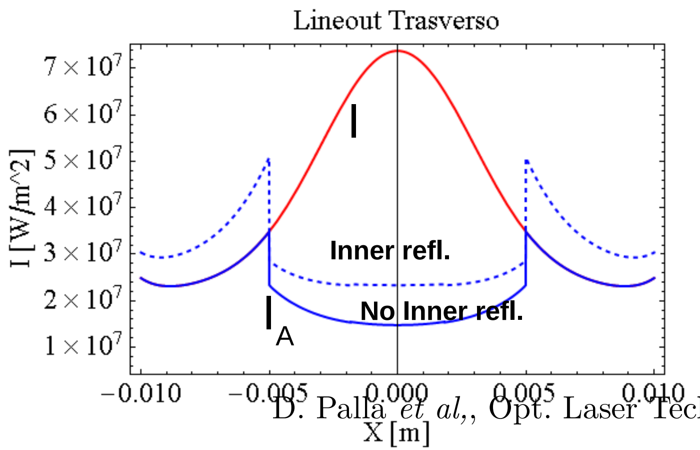

D. Palla *et al*,, Opt. Laser Techn. 156, 108524 (2022)

	Radial	Focus A	Focus B	Focus C
Sides	11	5	7	15
Diode Power (W)	40	45	35	70
Total diodes power (W)	440	450	490	2100
Focus (mm)	∞	15	15	80
Numerical aperture	0.17	0.17	0.17	0.17
% Power (doping radius)	57.6	58.5	58.2	82.8
% Power (extraction radius)	47.6	34.3	34.1	67.5
Optical Power (J/ms)	0.14	0.1	0.11	0.92

Multi-pulse extraction dynamics: rate equations (atomic) modelling

The role of the extraction by multiple pulses (made possible by the ~3.8ms lifetime) is being investigated using atomic physics modelling based on the rate equations

$$\frac{dn_i}{dt} = A_{ij}(t)\, n_j + B_{ijk}(t)\, n_j\, n_k$$

IEEE JOURNAL OF SELECTED TOPICS IN QUANTUM ELECTRONICS, VOL. 24, NO. 5, SEPTEMBER/OCTOBER 2018 1600713

Highly Efficient, Compact $Tm^{3+}:RE_2O_3$ (RE = Y, Lu, Sc) Sesquioxide Lasers Based on Thermal Guiding

Pavel Loiko, Philipp Koopmann, Xavier Mateos, Josep Maria Serres, Venkatesan Jambunathan, Antonio Lucianetti, Tomas Mocek, Magdalena Aguiló, Francesc Díaz, Uwe Griebner, Valentin Petrov, and Christian Kränkel

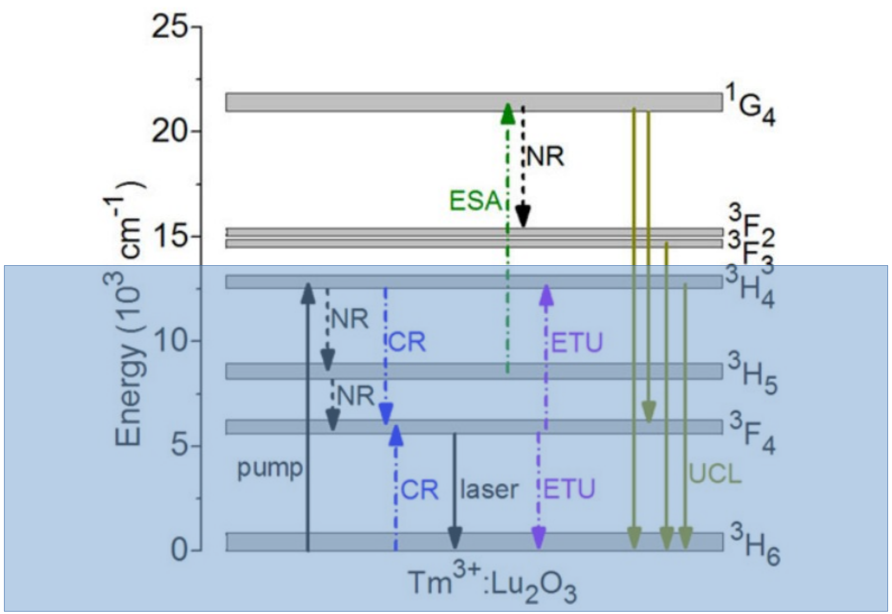

Fig. 1. Scheme of energy levels of the Tm^{3+} ion (on the example of $Tm^{3+}:Lu_2O_3$, C_2 site) showing relevant processes (CR: cross-relaxation, ETU: energy-transfer upconversion, ESA: excited-state absorption, UCL: upconversion luminescence, NR: non-radiative relaxation). The grey rectangles correspond to the total Stark splitting [30].

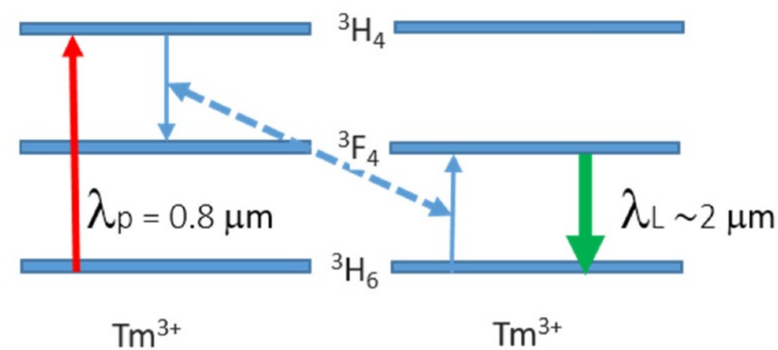

Figure 2. Scheme of the cross-relaxation (CR) process.

"two-for-one cross-relaxation mechanism"

overall quantum efficiency approaches 2 (beyond Stokes limit)

CNR-INO

Multi-pulse extraction dynamics: rate equations (atomic) modelling results

Rate equations (with transition rates based upon available data …) + “forced” extraction

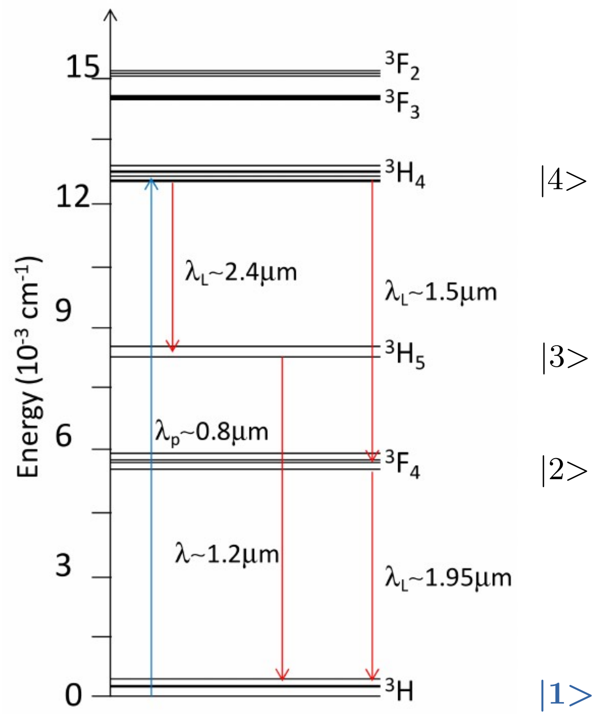

Figure 1. Energy level scheme of Tm^{3+} in Lu_2O_3 (ada

Two timescales involved: pumping/relaxation ~100us-1ms, extraction ~10ns

Extraction retrieved from a “lookup table” with results obtained using MIRO/COMMOD Pro simuations

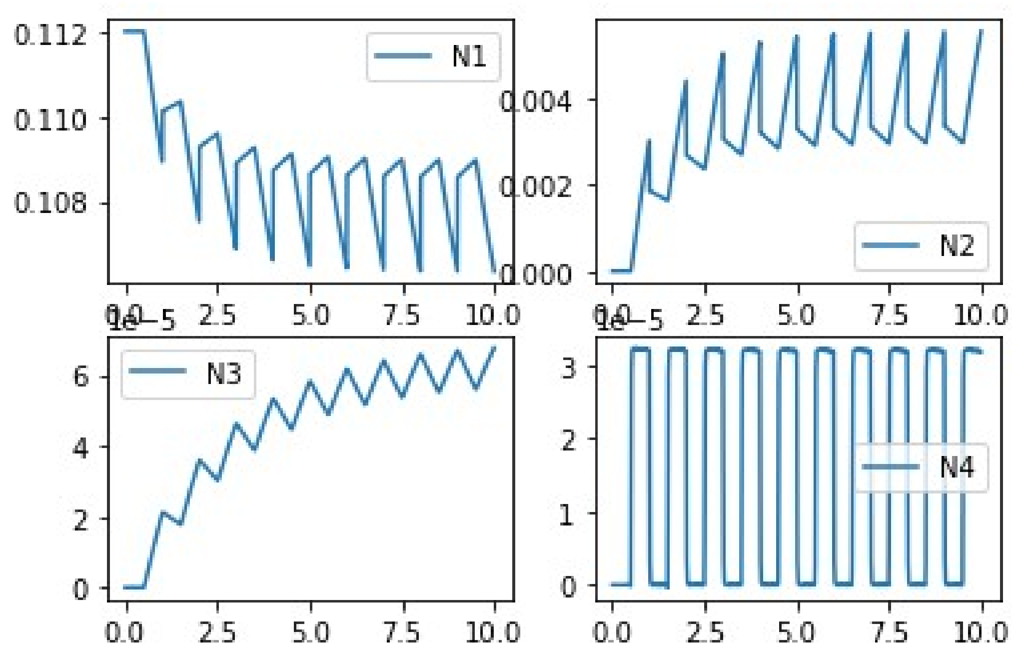

- Atomic dynamics simulations confirms MPE acts to reduce optical pump energy needs by a factor 2-3
- Role of CR critical and poorly assessed experimentally
- Effects of pump duty cycle not negligible for overall efficiency

CNR-INO

Ceramic Tm:Lu2O3 sample – laser test

A 5x5mm, 3mm thickness, 4%at Tm:Lu2O3 doped ceramic sample was recently acquired from Konoshima Baikowski. Laser properties studied at CNR-INO lab in Florence

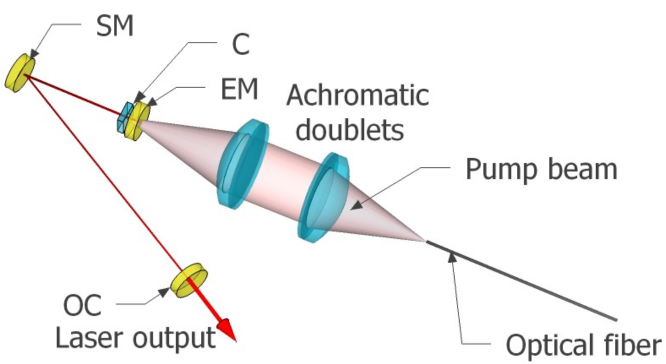

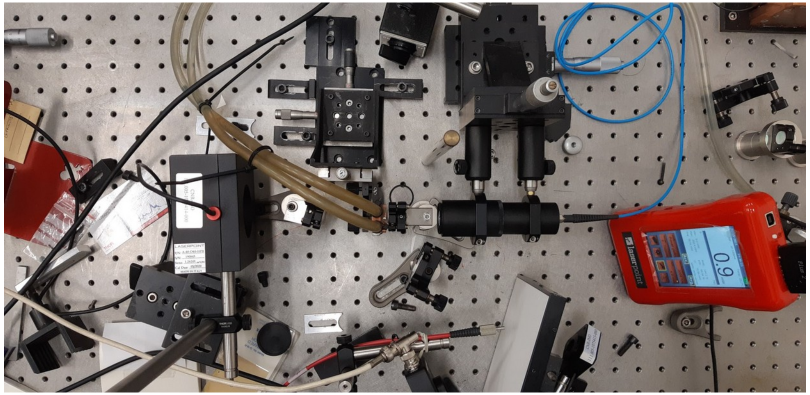

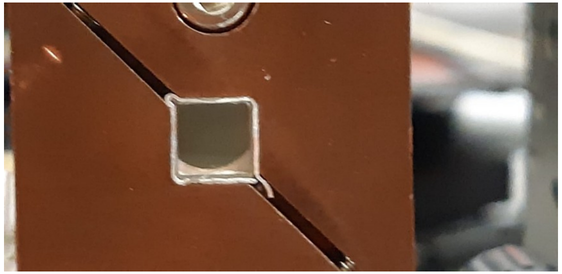

C: uncoated ceramics
EM: flat end mirror;
Total cavity length 170 mm

SM: spherical folding mirror (ROC 100 mm)
OC: flat output coupler mirror

SM and EM: high reflectivity @1.9-2.1 µm, high transmission @ 790 nm.

Pump laser: fiber coupled semiconductor laser, max output power 40 W, emission wavelength 790 nm.
QCW pumping, 10Hz, 10% DF

Pump spot: top hat, radius 50 µm, NA 0.22

Sample: Konoshima Tm:Lu2O3 ceramics, 4% doping, 5x5 mm, thickness 3.10 mm, no A/R coating

Laser emission results

Output power vs. absorbed pump power characterized with OC mirrors with different transmission T

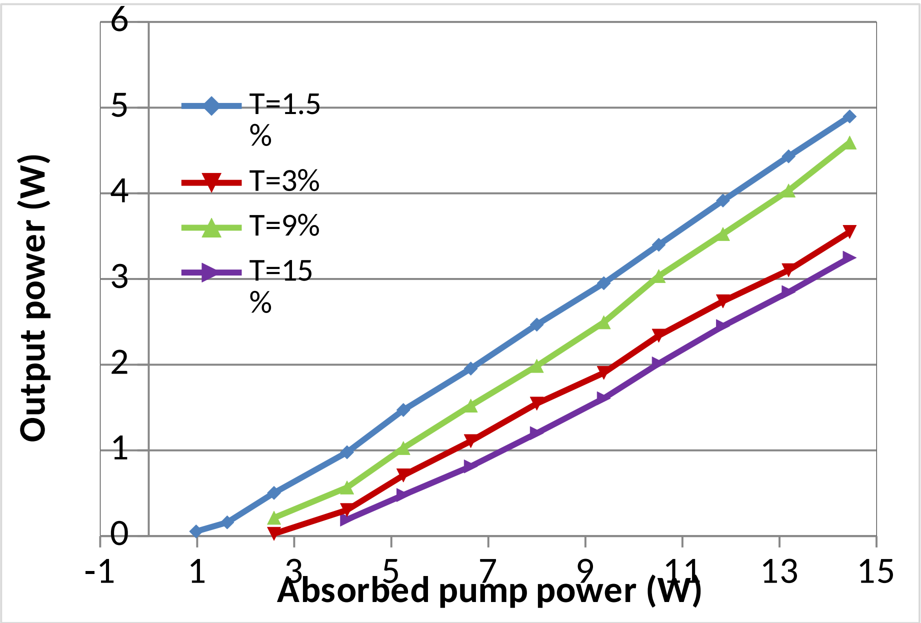

T	λ_{pk} (nm)	Slope Eff. (%)	Opt. Eff. (%)
1.5%	2063.6	38.0	33.9
3%	2060.8	31.6	24.6
9%	2053.4	40.3	31.8
15%	1954.3	32.1	22.4

Slope efficiency around 40% with all the OC mirrors, similar to other groups under semiconductor laser pumping (see for instance [1])

Slope efficiency comparable with the theoretical quantum efficiency $\lambda_{pump}/\lambda_{laser}$~40%

No clear indication on cross relaxation effects (i.e. “pay 1 pump photon, get 2 excited Tm ions”)

[1] P. Koopman et al., *Efficient diode-pumped laser operation of Tm:Lu2O3 around 2 μm*, Opt. Lett. 36, 6, 2011, p. 948

Laser emission: spectral properties vs. cavity losses

Laser emission spectra were characterized by means of a fiber coupled grating spectrometer (125 mm focal length) equipped with a 512 channels InGaAs array

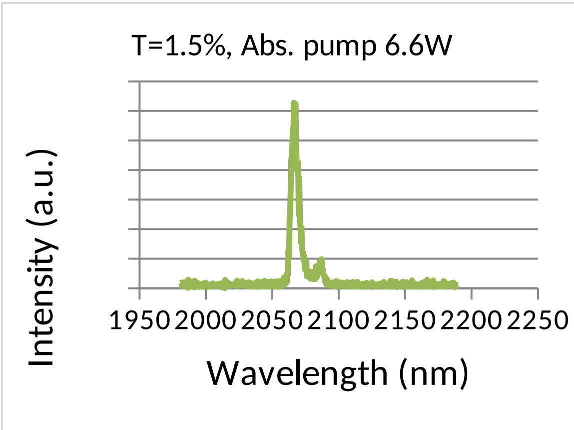

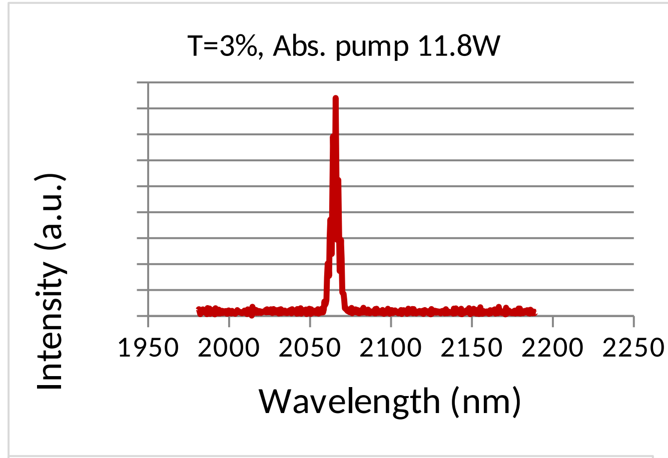

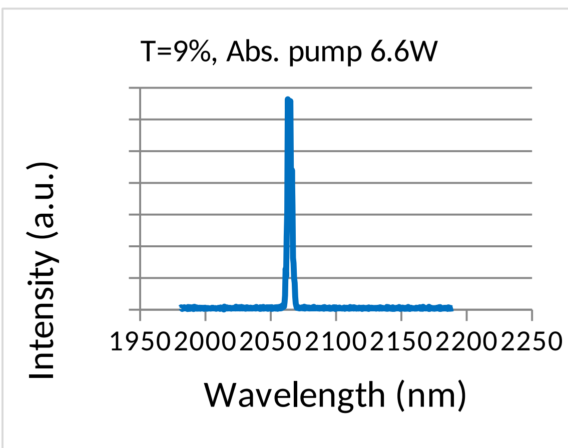

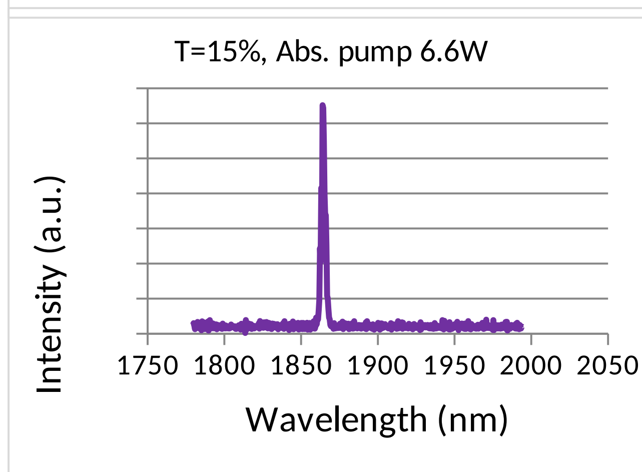

Blue shift of the emission wavelength for increasing cavity losses: typical *gain tuning* effect (see for instance C. Hönninger et al., Appl. Phys. B **69**, 3 (1999) for quasi-3 levels laser systems)

Measurement of absorption cross section

Absorption cross section on the ceramic sample has been measured using a spectrophotometer (Perkin Elmer Lambda25 UV/Vis Specrometer)

Optics

Beam center height	15 mm above cell holder bottom
Beam cross-section	1 nm slit ca. 0.6 mm x 9 mm (width x height) at focal point of sample and reference beam in sample compartment
Optical pathlength in sample compartment	121 mm
Grating (Monochromator)	Holographic concave grating with 1053 lines/mm in the center
Radiation sources	Prealigned deuterium and halogen lamps
Detector	Photodiodes (One for the sample beam and one for the reference beam)

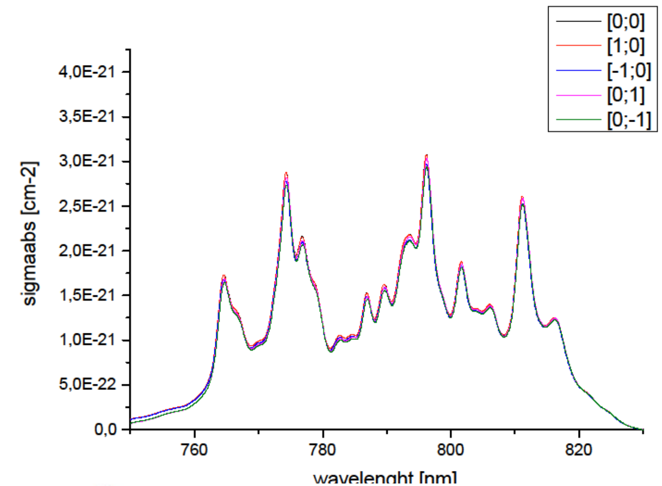

Different transverse positions

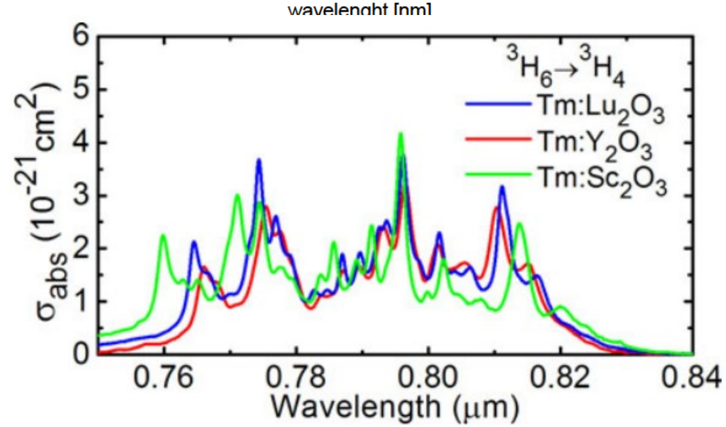

With respect to published result (with crystals), good shape agreement, ~20% absolute value reduction

Very good homogeneity across the sample

IEEE JOURNAL OF SELECTED TOPICS IN QUANTUM ELECTRONICS, VOL. 24, NO. 5, SEPTEMBER/OCTOBER 2018 1600713

Highly Efficient, Compact $Tm^{3+}:RE_2O_3$ (RE = Y, Lu, Sc) Sesquioxide Lasers Based on Thermal Guiding

Pavel Loiko, Philipp Koopmann, Xavier Mateos, Josep Maria Serres, Venkatesan Jambunathan,

Thermal management: numerical modelling

General properties:

- **Material:** $Tm^{3+}:Lu_2O_3$
- **Doping level:** 4%
- **Geometry:** Thin disk configuration (the doped active region is represented in yellow in the figure)
- **Thickness:** d=3 mm

Amplifier 1 (2X)
- R=6 mm
- r=2 mm
- E_o=130 mj
- E_p≈216 mj

Amplifier 2 (2X)
- R=6 mm
- r=4 mm
- E_o=320 mj
- E_p≈533 mj

Amplifier 3 (2X)
- R=15 mm
- r=8 mm
- E_o=1800 mj
- E_p≈3000 mj

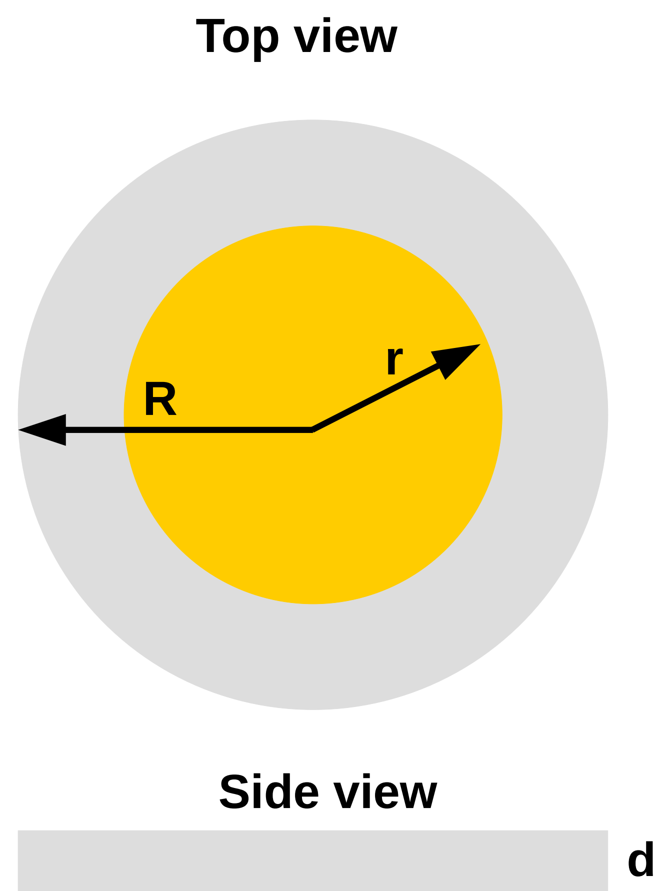

Pumping energy in the active medium (single pulse)

$$E_p = \underbrace{\eta_h E_p}_{heat} + \underbrace{(1-\eta_h) E_p}_{optical} \stackrel{\text{def}}{=} q + E_o$$

$$\eta_h \approx 0.4$$

$$q = \frac{\eta_h}{1-\eta_h} E_0$$

CNR-INO

Thermal management: numerical modelling

Heat distribution model

1) Idealized source

$$Q_o \stackrel{\text{def}}{=} \frac{E_p\,\eta_h\,\nu_L}{\pi r^2 d} \sim 2\times 10^9 \quad W/m^3$$

Q_0 is the order of magnitude of the power density at $\boldsymbol{\nu_L}$**=1 Khz** for amplifiers 1,2 and 3.

2) Map from pumping modelling

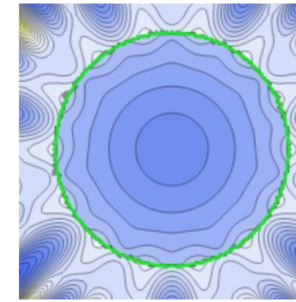

Power density Q is calculated for an a given configuration.

Heat Trasfer Equation

FEM numerical solution (using Mathematica)

$$\rho\, C_P\, \partial_t T(t,\mathbf{x}) + \nabla\cdot\left[-k\, T(t,\mathbf{x})\,\nabla T(t,\mathbf{x})\right] = Q(t,\mathbf{x})$$

Neumann contition on spatial boundaries

$$\frac{\partial T}{\partial n} = \frac{h}{k}\left[T_{\text{ext}}(t,\mathbf{x}) - T(t,\mathbf{x})\right]$$

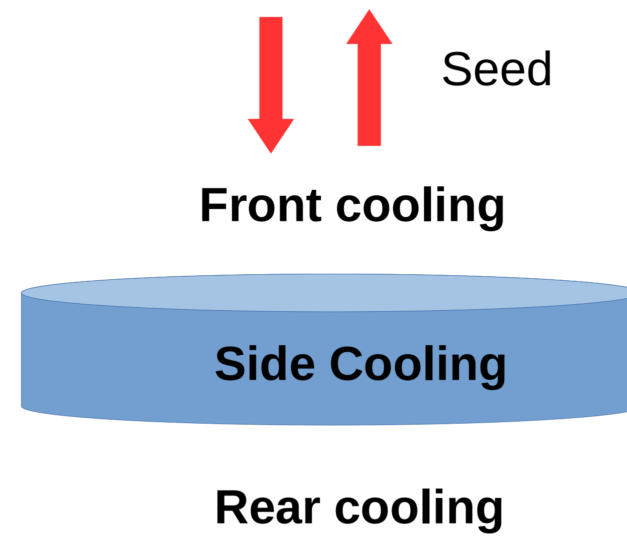

Thermal management: general params/architecture

Active medium parameters

- Density: 9.33 g/cm³
- Specific heat capacity: **c_p=0.24 J/gK**
- Thermal conductivity: **k=12.3 W/mK**
- Intensity: **≈0.6 J/cm²**

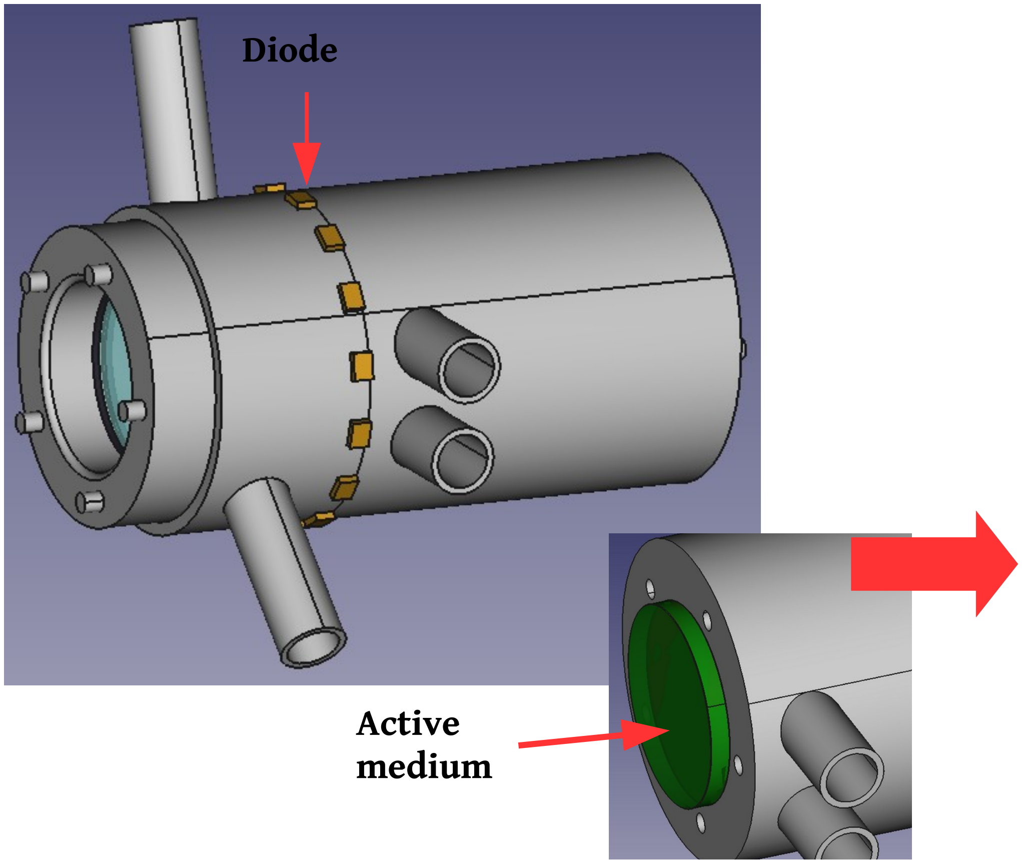

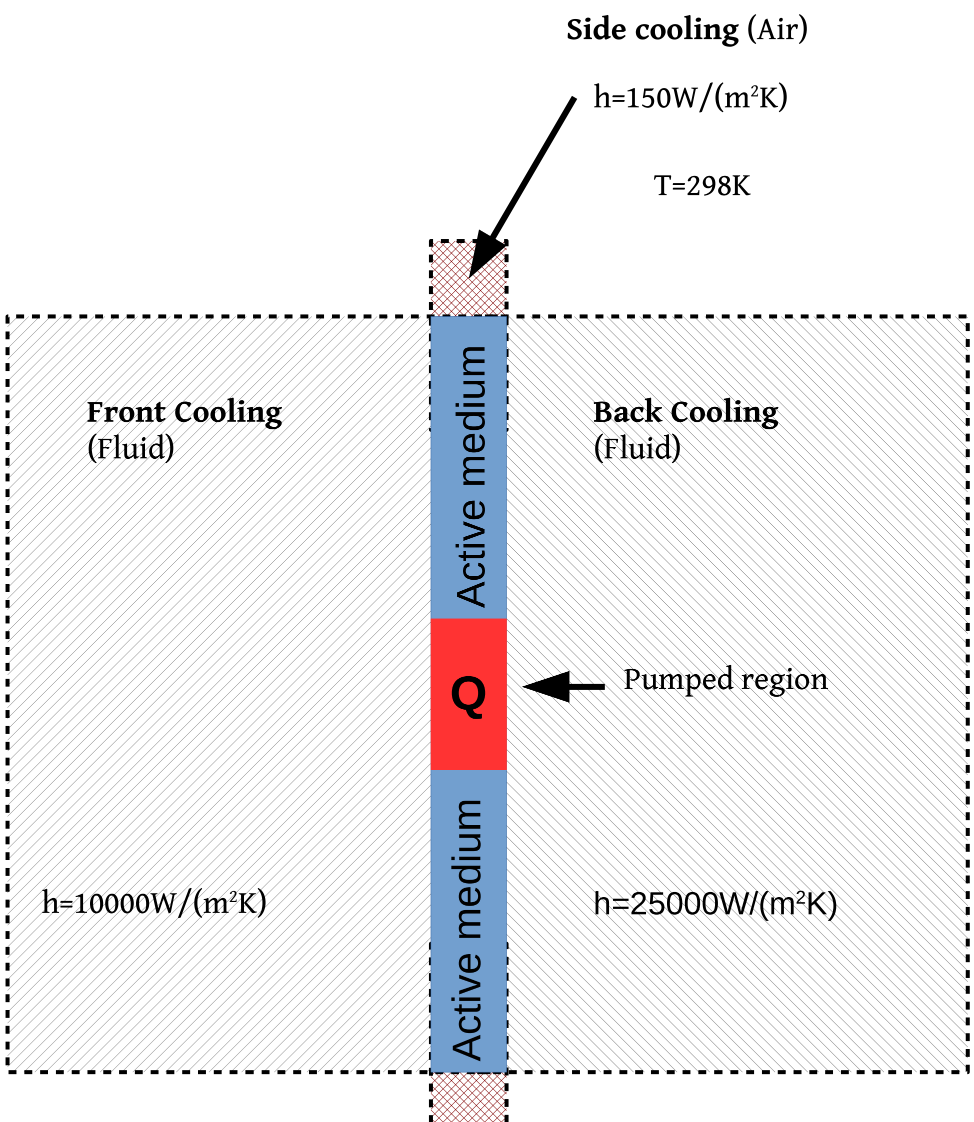

Thermal management: results for amplifier 3

Longitudinal doping/pumping tailoring

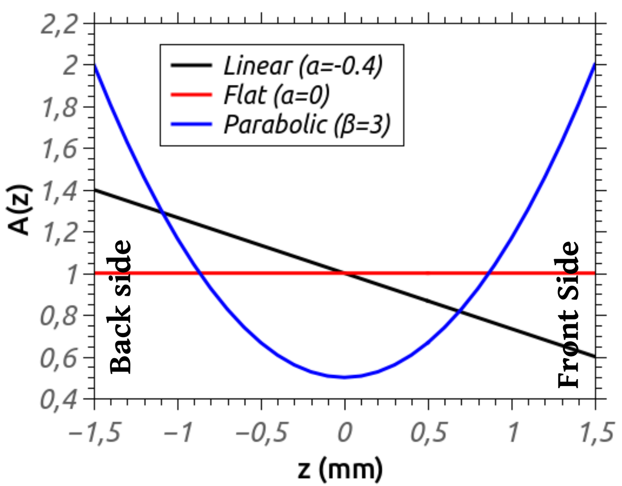

T(z) at x=y=0 in steady state conditions

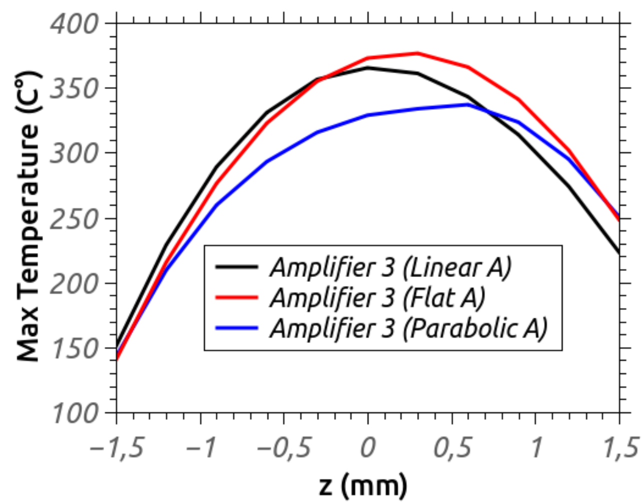

T(t) at x=y=0 (source is turn on at t=0)

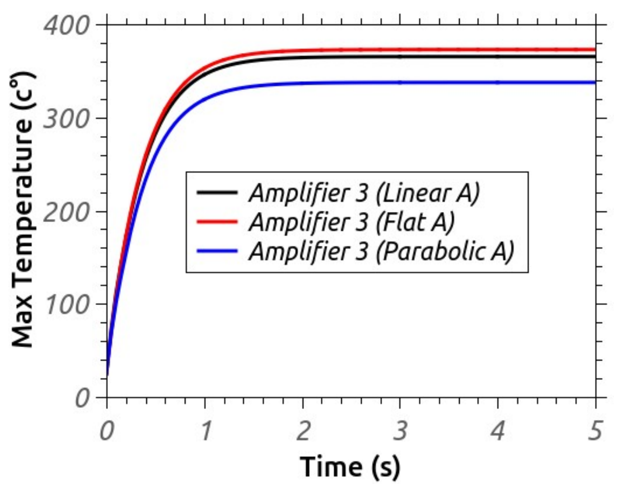

- At a fixed total power, it is clearly convenient to concentrate the power density (i.e. the doping concentration) on the cooled surfaces
- Note that frontal and back cooling are different and thus a linear power density distribution can be effective in reducing maximum temperature.
- The system becomes stationary in ~1s time

Thermal management: results for amplifier 3

Front Face (z=1.5 mm)

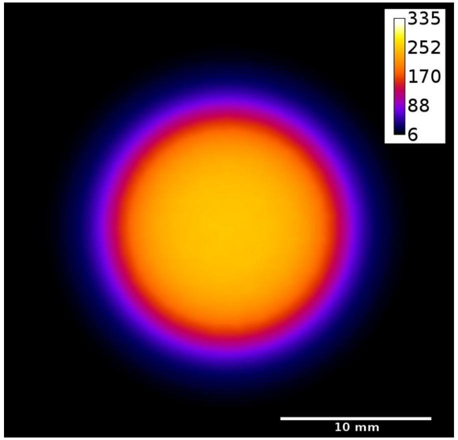

Z=0.6 mm

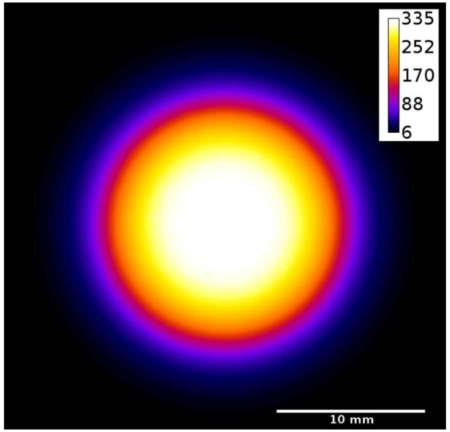

Back face (z=-1.5 mm)

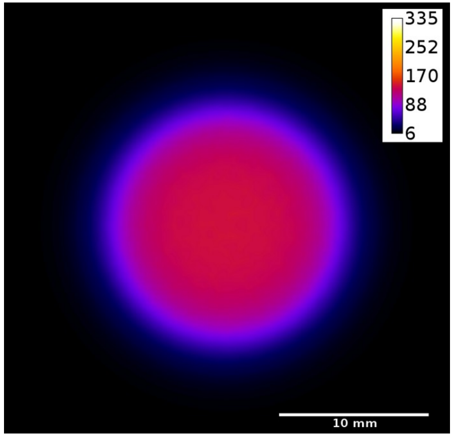

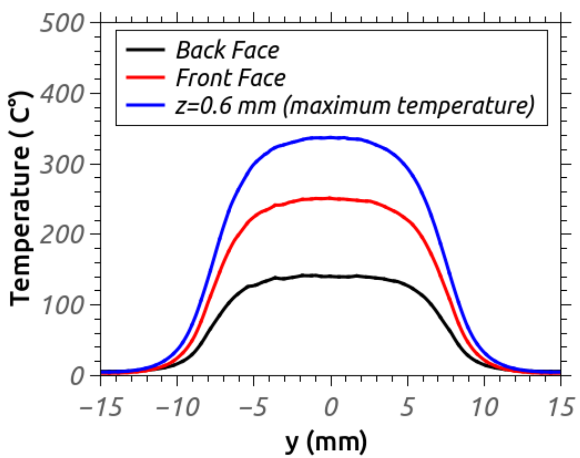

With a parabolic heat distribution we decrease the density power on the inner disk regions, which are the most difficult to be cooled due the low thermal conductivity. In case of a single cooled face, however, it is convenient to adopt an exponential-like distribution:

$$A(z)=\frac{\alpha}{1-e^{-\alpha}}e^{-\frac{\alpha}{d}(z+d/2)}$$

CNR-INO

MIXED OXIDES AND SESQUIOXIDES

Solid solutions of hosts with compatible lattice structure. The internal disordered structure may induce an inhomogeneous broadening on the absorption and emission spectra of the optically active ion (i.e. Yb3+, Tm3+, Nd3+) due to the changing Stark splitting from site to site.

Pure matrices	Substitution	Mixed matrices
• $Y_3Al_5O_{12}$=YAG	Y^{3+} → Lu^{3+}	• LuYAG
• GGG	Ga^{3+} → Al^{3+}	• GAGG
• YAG	Al^{3+} → Sc^{3+}	• YSAG
• Y_2O_3	Y^{3+} → Lu^{3+}	• $(Lu,Y)_2O_3$
• Sc_2O_3	Sc^{3+} → Y^{3+}	• $(Sc_2\ ,Y)O_3$

Broadband tuning, generation and amplification of ultrashort laser pulses

A. Pirri, G. Toci, *et al.*, Materials 11, 837 (2018)

A. Pirri et al., Materials 15, 2084 (2022)

Courtesy of A. Pirri

materials

MDPI

Review

Achievements and Future Perspectives of the Trivalent Thulium-Ion-Doped Mixed-Sesquioxide Ceramics for Laser Applications

Angela Pirri [1,*], Roman N. Maksimov [2,3], Jiang Li [4,5], Matteo Vannini [6] and Guido Toci [6]

1 Istituto di Fisica Applicata "N. Carrara", Consiglio Nazionale delle Ricerche, 50019 Sesto Fiorentino, FI, Italy
2 Institute of Electrophysics UrB RAS, 620016 Ekaterinburg, Russia; romanmaksimov@e1.ru
3 Ural Federal University Named after the First President of Russia B.N. Yeltsin, 620002 Ekaterinburg, Russia
4 Key Laboratory of Transparent Opto-Functional Inorganic Materials, Shanghai Institute of Ceramics, Chinese Academy of Sciences, Shanghai 201899, China; lijiang@mail.sic.ac.cn
5 Center of Materials Science and Optoelectronics Engineering, University of Chinese Academy of Sciences, Beijing 100049, China
6 Istituto Nazionale di Ottica, Consiglio Nazionale delle Ricerche, INO-CNR, 50019 Sesto Fiorentino, FI, Italy; matteo.vannini@ino.cnr.it (M.V.); guido.toci@ino.cnr.it (G.T.)
* Correspondence: a.pirri@ifac.cnr.it; Tel.: +39-055-522-5318

Abstract: This paper is devoted to reviewing the latest results achieved in solid-state lasers based on thulium-doped mixed-sesquioxide ceramics, i.e., $(Lu,Sc,Y)_2O_3$. The near- and mid-infrared regions are of interest for many applications, from medicine to remote sensing, as they match molecular fingerprints and cover several atmospheric transparency windows. These matrices are characterized by a strong electron–phonon interaction—which results in a large splitting of the ground

A. Pirri, *et al.*, Materials 15(6), 2084, (2022)

Table 3. Data obtained in the pulsed regime of the mixed ceramics reported in the literature; λ_L: laser wavelength emission; P_{out}: laser output power; τ_L: pulse duration; *f*: repetition rate.

Sample	λ_L (nm)	P_{out} (mW)	τ_L (fs)	*f* (MHz)	Ref.
$LuScO_3$	1975	32	590 ps	34.72	[55]
$Lu_{2/3}Sc_{1/3}O_3$	2057	30	63	78.9	[54]
$Lu_{2/3}Sc_{1/3}O_3$	2081	220	58	84.8	[56]
$LuYO_3$	2048	51	54	78	[52]
$LuYO_3$	2045	63	57	72.6	[59]
$LuYO_3$	2061	121	410	139.3	[147]
$LuYO_3$	2047	540	120.3 ns	26.31	[51]
$LuScO_3^c$	2093	113	170	115.2	[146]

Table 2. CW and *quasi*-CW laser performance of the mixed ceramics reported in the literature; P_{out}: laser output power; λ_L: laser wavelength emission; η: slope efficiency; P_{th}: laser threshold.

Sample	Doping *at.%*	P_{out} (W)	λ_L (nm)	η (%)	P_{th} (W)	Ref.
$LuScO_3$	2	0.211	1982	8.2	0.840	[55]
$(Lu_{2/3}Sc_{1/3})_2O_3$	4.76	1	2100	24	0.860	[121]
$Lu_{1.6}Sc_{0.4}O_3$	1	9.8	2090	40	2.8	[54]
$Lu_{1.6}Sc_{0.4}O_3$	1.5	11	2090	39	5.0	[54]
$Lu_{0.8}Sc_{0.2}O_3$	2	1.88	2090	24.6	3.2	[122]
$(Lu_{2/3}Sc_{1/3})_2O_3$	2.8	0.490	2088	26.8	-	[56]
$LuYO_3$	3	1.55	2050	19.9	1.1	[51]
$LuYO_3$	3	1.20	2067	25.1	0.530	[147]
$LuYO_3$	3	0.440	2074	-	0.140	[59]
YO_3	3	0.603	2060	33.2	0.250	[52]
$LuYO_3$	3	0.600	2076	11.5	0.250	[52]
$(Sc_{1/4}Y_{3/4})O_3$	5	1.24	2077	9.45	3.49	[53]
$LuScO_3$ crystal	1	0.250	1982	55	0.038	[143]
$LuScO_3$ crystal	1	0.705	2100	55	0.038	[143]

A. Pirri et al., Materials 15, 2084 (2022)

Table 1. Spectroscopic data on the mixed ceramics reported in the literature; λ_{abs} and λ_{em} are the wavelengths at which the absorption and emission cross-sections were calculated, respectively.

Sample	Doping *at.%*	σ_{abs} ($\times 10^{-21}$ cm^{-2})	λ_{abs} (nm)	σ_{em} ($\times 10^{-21}$ cm^{-2})	λ_{em} (nm)	Grain Size (μm)	Lattice Const. (Å)	Ref.
$LuScO_3$	2	3.5	793	-		1.65		[55]
$(Lu_{2/3}Sc_{1/3})_2O_3$	4.76	2.8	793	7.15	1951	4–5	10.3683	[121]
$(Lu_{2/3}Sc_{1/3})_2O_3$	4.76	4.2	1622	2.38	2090			[121]
$Lu_{1.6}Sc_{0.4}O_3$	1.5	3.1	796	1.11	2090	1.54		[54]
$Lu_{0.8}Sc_{0.2}O_3$	2	-		-		2.5		[122]
$(Lu_{2/3}Sc_{1/3})_2O_3$	2.8	-		7.0	1950	-	-	[56]
$LuYO_3$	3	3.8	796	6.0	1937	1.65	-	[51]
$LuYO_3$	3	3.0	2055	-		1.65	-	[147]
$LuScO_3$ crystal	1	2.6	793	8.0	1956	-	10.105	[143]
$(Sc_{1/4}Y_{3/4})_2O_3$	5			3.9	2098	28.2	10.401	[53]

Courtesy of A. Pirri

Summary and conclusions

- Conceptual design of a <100fs, >500mJ, 1kHz amplification chain based on Tm:Lu2O3 carried out; technical design ongoing

- Optical amplification simulations predict an extraction efficiency up to ~10% so far (role of MPE still under investigation)

- (Direct) diode pumping optical configuration studied, showing a pretty homogeneous pumping distribution can be obtained by a suitable tuning of diode (bar) number, focusing, ...

- Extraction dynamics (MPE) under investigation, shows room for pump energy/power optimization (~2x)
  Experimental investigation of transition rates and CR rates needed/in planning

- Perspectives for shorter pulses using mixed sesquioxides

- Thermal management: FEM modelling setup
  - longitudinal tailoring of doping needed to reduce maximum temperature/gradients
  - cooling on both surfaces possibly needed (still under investigation)
  - precise knowledge of thermal conductivity (and dependence on T) – few data available

- Experimental characterization of a 4at% ceramic sample:
  - Absorption cross section measured, closely resembling (few) available data
  - Slope efficiency in line with predictions/available data; role of cross relaxation still to be investigated (need for dedicated measurements)

CNR-INO

Table IV: Laser parameters for an LPA-based 1-TeV linear collider operating at $n=10^{17}$ cm^{-3}.

	~1 micron laser wavelength	2 micron laser wavelength	Plasma density (n) & laser wavelength (λ) scalings
Energy [J]	6.5	1.6	$n^{-3/2}\,\lambda^{-2}$
I [10^{18} W/cm^2]	2	0.5	λ^{-2}
Duration, FWHM [fs]	130	130	$n^{-1/2}$
Peak power [TW]	50	12	$n^{-1}\,\lambda^{-2}$
Rep. rate [kHz]	47	47	n
Average power [kW]	310	75	$n^{-1/2}\,\lambda^{-2}$
LPA stages / linac	100	400	$n\,\lambda^{2}$
Efficiency [%]	>30	>30	-
Contrast	10^6	10^5	λ^{-2}

Report on Laser Technologies for kBELLA and beyond (2017)
C. Schroeder *et al.*, Phys. Rev. Spec. Top. Accel. Beams 13, 101301 (2010)